6. S. R. Marder, C. B. Gorman, B. G. Tiemann, L.-T. Cheng, *Proc. SPIE* **1775**, 19 (1993); C. B. Gorman and S. R. Marder, in preparation.
7. W. Drenth and E. E. Wiebenga, *Acta Crystallogr.* **8**, 755 (1955).
8. R. H. Baughman, B. E. Kohler, I. J. Levy, C. W. Spangler, *Synth. Methods* **11**, 37 (1985).
9. P. Groth, *Acta Chem. Scand. B* **41**, 547 (1987).
10. F. Chentli-Bechikha, J. P. Declercq, G. Germain, M. V. Meerssche, *Cryst. Struct. Comm.* **6**, 421 (1977).
11. L. G. S. Brooker *et al.*, *J. Am. Chem. Soc.* **73**, 5332 (1951).
12. R. Radeglia and S. Dähne, *J. Mol. Struct.* **5**, 399 (1970).
13. S. R. Marder *et al. J. Am. Chem. Soc.* **115**, 2525 (1993).
14. S. Schneider, *Ber. Buns. Ges.* **80**, 218 (1976).
15. H. E. Schaffer, R. R. Chance, R. J. Silbey, K. Knoll, R. R. Schrock, *J. Chem. Phys.* **94**, 4161 (1991).
16. F. Kajzar and J. Messier, *Rev. Sci. Instrum.* **58**, 2081 (1987).
17. S. R. Marder, J. W. Perry, F. L. Klavetter, R. H. Grubbs, in *Organic Materials for Nonlinear Optics*, R. A. Hann and D. Bloor, Eds. (Royal Society of Chemistry, London, 1989), pp. 288–294.
18. F. Kajzar, in *Nonlinear Optics of Organics and Semiconductors*, T. Kobayashi, Ed. (Springer-Verlag, Berlin, 1989), pp. 108–119.
19. S. H. Stevenson, D. S. Donald, G. R. Meredith, in *Nonlinear Optical Properties of Polymers*, *Mat. Res. Soc. Symp. Proc. 109* (Materials Research Society, Pittsburgh, 1988), pp. 103–108.
20. Y. Marcus, *J. Soln. Chem.* **20**, 929 (1991).
21. B. M. Pierce, *Proc. SPIE* **1560**, 148 (1991).
22. C. W. Dirk, L.-T. Cheng, M. G. Kuzyk, *Int. J. Quant. Chem.* **43**, 27 (1992).
23. Enhancement of γ by the P2 term has been discussed previously: A. F. Garito, J. R. Heflin, K. Y. Yong, O. Zamani-khamiri, *Proc. SPIE* **971**, 2 (1988).
24. Increased γ in donor-acceptor–conjugated organics relative to centrosymmetric analogs has been observed experimentally: C. W. Spangler, K. O. Havelka, M. W. Becker, T. A. Kelleher, L.-T. Cheng, *Proc. SPIE* **1560**, 139 (1991); L.-T. Cheng *et al.*, *J. Phys. Chem.* **95**, 10631 (1991); L.-T. Cheng *et al.*, *ibid.*, p. 10643.
25. The research was performed, in part, at the Center for Space Microelectronics Technology, Jet Propulsion Laboratory (JPL), California Institute of Technology, and was supported, in part, by the Strategic Defense Initiative Organization–Innovative Science and Technology Office, through an agreement with the National Aeronautics and Space Administration (NASA). Support at the Beckman Institute by the Air Force Office of Scientific Research (grant F49620-92-J-0177) is also acknowledged. C.B.G. thanks the JPL director's office for a postdoctoral fellowship. G.B. thanks the National Research Council and NASA for a resident research associateship at JPL.

29 January 1993; accepted 19 May 1993

Complex Patterns in a Simple System

John E. Pearson

Numerical simulations of a simple reaction-diffusion model reveal a surprising variety of irregular spatiotemporal patterns. These patterns arise in response to finite-amplitude perturbations. Some of them resemble the steady irregular patterns recently observed in thin gel reactor experiments. Others consist of spots that grow until they reach a critical size, at which time they divide in two. If in some region the spots become overcrowded, all of the spots in that region decay into the uniform background.

Patterns occur in nature at scales ranging from the developing *Drosophila* embryo to the large-scale structure of the universe. At the familiar mundane scales we see snowflakes, cloud streets, and sand ripples. We see convective roll patterns in hydrodynamic experiments. We see regular and almost regular patterns in the concentrations of chemically reacting and diffusing systems (*1*). As a consequence of the enormous range of scales over which pattern formation occurs, new pattern formation phenomenon is potentially of great scientific interest. In this report, I describe patterns recently observed in numerical experiments on a simple reaction-diffusion model. These patterns are unlike any that have been previously observed in theoretical or numerical studies.

The system is a variant of the autocatalytic Selkov model of glycolysis (*2*) and is due to Gray and Scott (*3*). A variety of spatio-temporal patterns form in response

to finite-amplitude perturbations. The response of this model to such perturbations was previously studied in one space dimension by Vastano *et al.* (*4*), who showed that steady spatial patterns could form even when the diffusion coefficients were equal. The response of the system in one space dimension is nontrivial and depends both on the control parameters and on the initial perturbation. It will be shown that the patterns that occur in two dimensions range from the well-known regular hexagons to irregular steady patterns similar to those recently observed by Lee *et al.* (*5*) to chaotic spatio-temporal patterns. For the ratio of diffusion coefficients used, there are no stable Turing patterns.

Most work in this field has focused on pattern formation from a spatially uniform state that is near the transition from linear stability to linear instability. With this restriction, standard bifurcation-theoretic tools such as amplitude equations have been developed and used with considerable success (*6*). It is unclear whether the pat-

terns presented in this report will yield to these now-standard technologies.

The Gray-Scott model corresponds to the following two reactions:

$$U + 2V \rightarrow 3V \qquad (1)$$
$$V \rightarrow P$$
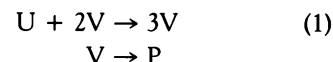
Both reactions are irreversible, so P is an inert product. A nonequilibrium constraint is represented by a feed term for U. Both U and V are removed by the feed process. The resulting reaction-diffusion equations in dimensionless units are:

$$\frac{\partial U}{\partial t} = D_u \nabla^2 U - UV^2 + F(1 - U)$$

$$\frac{\partial V}{\partial t} = D_v \nabla^2 V + UV^2 - (F + k)V \quad (2)$$

where k is the dimensionless rate constant of the second reaction and F is the dimensionless feed rate. The system size is 2.5 by 2.5, and the diffusion coefficients are $D_u = 2 \times 10^{-5}$ and $D_v = 10^{-5}$. The boundary conditions are periodic. Before the numerical results are presented, consider the behavior of the reaction kinetics which are described by the ordinary differential equations that result upon dropping the diffusion terms in Eq. 2.

In the phase diagram shown in Fig. 1, a trivial steady-state solution $U = 1, V = 0$ exists and is linearly stable for all positive F and k. In the region bounded above by the solid line and below by the dotted line, the system has two stable steady states. For fixed k, the nontrivial stable uniform solution loses stability through saddle-node bifurcation as F is increased through the upper solid line or by Hopf bifurcation to a periodic orbit as F is decreased through the dotted line. [For a discussion of bifurcation theory, see chapter 3 of (*7*).] In the case at hand, the bifurcating periodic solution is stable for $k < 0.035$ and unstable for $k > 0.035$. There are no periodic orbits for parameter values outside the region enclosed by the solid line. Outside this region the system is excitable. The trivial state is linearly stable and globally attracting. Small perturbations decay exponentially but larger perturbations result in a long excursion through phase space before the system returns to the trivial state.

The simulations are forward Euler integrations of the finite-difference equations resulting from discretization of the diffusion operator. The spatial mesh consists of 256 by 256 grid points. The time step used is 1. Spot checks made with meshes as large as 1024 by 1024 and time steps as small as 0.01 produced no qualitative difference in the results.

Initially, the entire system was placed in the trivial state ($U = 1, V = 0$). The 20 by 20 mesh point area located symmetrically

Center for Nonlinear Studies, Los Alamos National Laboratory, Los Alamos, NM 87545.

about the center of the grid was then perturbed to ($U = 1/2, V = 1/4$). These conditions were then perturbed with ±1% random noise in order to break the square symmetry. The system was then integrated for 200,000 time steps and an image was saved. In all cases, the initial disturbance propagated outward from the central square, leaving patterns in its wake, until the entire grid was affected by the initial square perturbation. The propagation was wave-like, with the leading edge of the perturbation moving with an approximately constant velocity. Depending on the parameter values, it took on the order of 10,000 to 20,000 time steps for the initial perturbation to spread over the entire grid. The propagation velocity of the initial perturbation is thus on the order of 1×10^{-4} space units per time unit. After the initial period during which the perturbation spread, the system went into an asymptotic state that was either time-independent or time-dependent, depending on the parameter values.

Figures 2 and 3 are phase diagrams; one can view Fig. 3 as a map and Fig. 2 as the key to the map. The 12 patterns illustrated in Fig. 2 are designated by Greek letters. The color indicates the concentration of U with red representing $U = 1$ and blue representing $U \approx 0.2$; yellow is intermediate to red and blue. In Fig. 3, the Greek characters indicate the pattern found at that point in parameter space. There are two additional symbols in Fig. 3, R and B, indicating spatially uniform red and blue states, respectively. The red state corresponds to ($U = 1, V = 0$) and the blue state depends on the exact parameter values but corresponds roughly to ($U = 0.3, V = 0.25$).

Pattern α is time-dependent and consists of fledgling spirals that are constantly colliding and annihilating each other: full spirals never form. Pattern β is time-dependent and consists of what is generally called phase turbulence (8), which occurs in the vicinity of a Hopf bifurcation to a stable periodic orbit. The medium is unable to synchronize so the phase of the oscillators varies as a function of position. In the present case, the small-amplitude periodic orbit that bifurcates is unstable. Pattern γ is time-dependent. It consists primarily of stripes but there are small localized regions that oscillate with a relatively high frequency ($\sim 10^{-3}$). The active regions disappear, but new ones always appear elsewhere. In
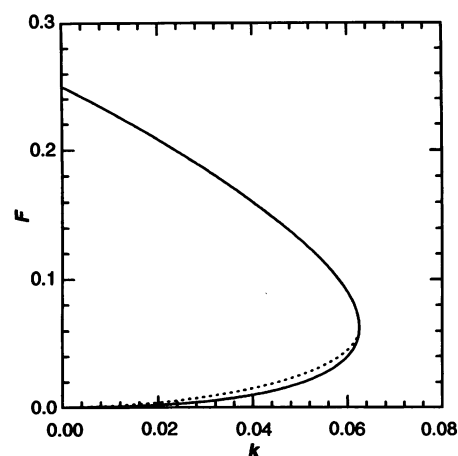

Fig. 2. The key to the map. The patterns shown in the figure are designated by Greek letters, which are used in Fig. 3 to indicate the pattern found at a given point in parameter space.

Fig. 1. Phase diagram of the reaction kinetics. Outside the region bounded by the solid line, there is a single spatially uniform state (called the trivial state) ($U = 1, V = 0$) that is stable for all (F, k). Inside the region bounded by the solid line, there are three spatially uniform steady states. Above the dotted line and below the solid line, the system is bistable: There are two linearly stable steady states in this region. As F is decreased through the dotted line, the non-trivial stable steady state loses stability through Hopf bifurcation. The bifurcating periodic orbit is stable for $k < 0.035$ and unstable for $k > 0.035$. No periodic orbits exist for parameter values outside the region bounded by the solid line.
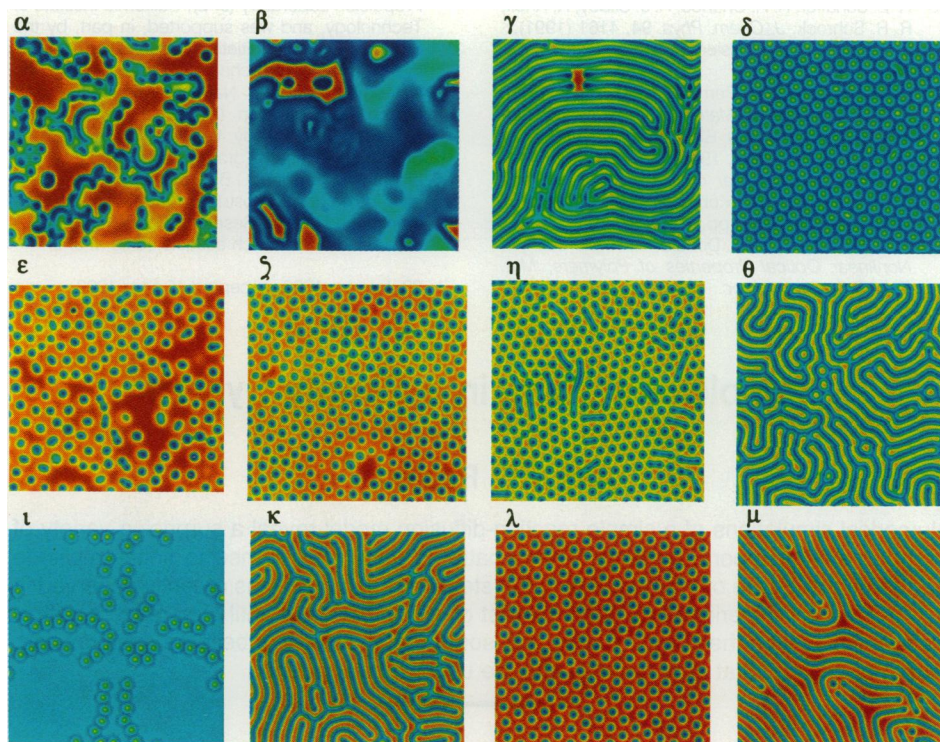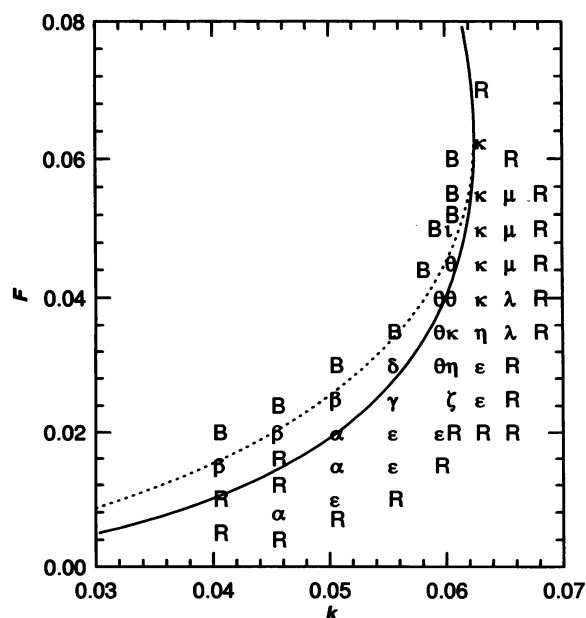

Fig. 3. The map. The Greek letters indicate the location in parameter space where the patterns in Fig. 2 were found; B and R indicate that the system evolved to uniform blue and red states, respectively.

Fig. 2 there is an active region near the top center of pattern γ. Pattern δ consists of regular hexagons except for apparently stable defects. Pattern η is time-dependent: a few of the stripes oscillate without apparent decay, but the remainder of the pattern remains time-independent. Pattern ι is time-dependent and was observed for only a single parameter value.

Patterns θ, κ, and μ resemble those observed by Lee *et al.* (5). When blue waves collide, they stop, as do those observed by Lee *et al.* In pattern μ, long stripes grow in length. The growth is parallel to the stripes and takes place at the tips. If two distinct stripes that are both growing are pointed directly at each other, it is always observed that when the growing tips reach some critical separation distance, they alter their course so as not to collide. In patterns θ and κ, the perturbations grow radially outward with a velocity normal to the stripes. In these cases if two stripes collide, they simply stop, as do those observed by Lee *et al.* I have also observed, in one space dimension, fronts propagating toward each other that stop when they reach a critical separation. This is fundamentally new behavior for nonlinear waves that has recently been observed in other models as well (9).

Patterns ε, ζ, and λ share similarities. They consist of blue spots on a red or yellow background. Pattern λ is time-independent and patterns ε and ζ are time-dependent. Note that spots occur only in regions of

parameter space where the system is excitable and the sole uniform steady state is the red state ($U = 1, V = 0$). Thus, the blue spots cannot persist for extended time unless there is a gradient present. Because the gradient is required for the existence of the spots, they must have a maximum size or there would be blue regions that were essentially gradient-free. Such regions would necessarily decay to the red state. Note that these gradients are self-sustaining and are not imposed externally. After the initial perturbation, the spots increase in number until they fill the system. This process is visually similar to cell division. After a spot has divided to form two spots, they move away from each other. During this period, each spot grows radially outward. The growth is a consequence of excitability. As the spots get further apart, they begin to elongate in the direction perpendicular to their motion. When a critical size is achieved, the gradient is no longer sufficient to maintain the center in the blue state, so the center decays to red, leaving two blue spots. This process is illustrated in Fig. 4. Figure 4A was made just after the initial square perturbation had decayed to leave the four spots. In Fig. 4B, the spots have moved away from each other and are beginning to elongate. In Fig. 4C, the new spots are clearly visible. In Fig. 4D, the replication process is complete. The subsequent evolution depends on the control parameters. Pattern λ remains in a steady state. Pattern ζ

remains time-dependent but with long-range spatial order except for local regions of activity. The active regions are not stationary. At any one instant, they do not appear qualitatively different from pattern ζ (Fig. 2) but the location of the red disturbances changes with time. Pattern ε appears to have no long-range order either in time or space. Once the system is filled with blue spots, they can die due to overcrowding. This occurs when many spots are crowded together and the gradient over an extended region becomes too weak to support them. The spots in such a region will collapse nearly simultaneously to leave an irregular red hole. There are always more spots on the boundary of any hole, and after a few thousand time steps no sign of the hole will remain. The spots on its border will have filled it. Figure 5 illustrates this process.

Pattern ε is chaotic. The Liapunov exponent (which determines the rate of separation of nearby trajectories) is positive. The Liapunov time (the inverse of the Liapunov exponent) is 660 time steps, roughly equal to the time it takes for a spot to replicate, as shown in Fig. 4. This time period is also about how long it takes for a molecule to diffuse across one of the spots. The time average of pattern ε is constant in space.

All of the patterns presented here arose in response to finite-amplitude perturbations. The ratio of diffusion coefficients used was 2. It is now well known that Turing instabilities that lead to spontaneous pattern
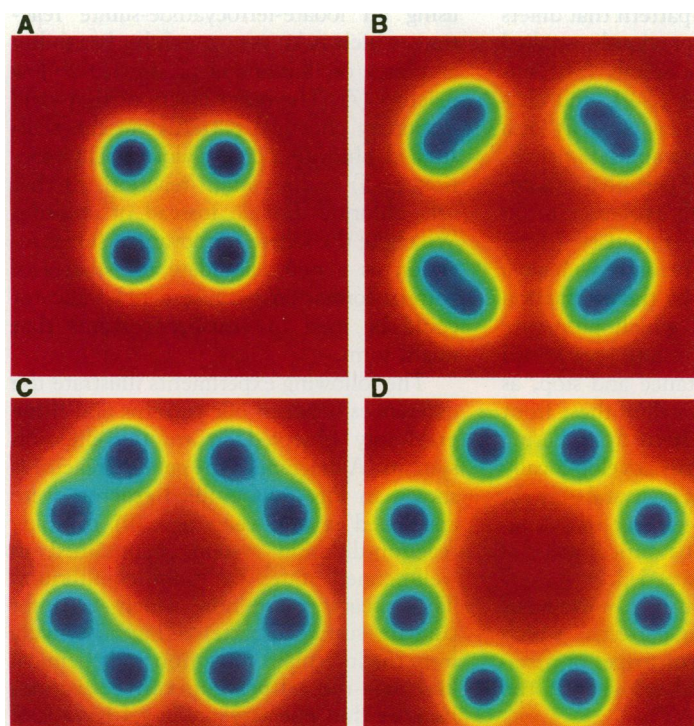
Fig. 4 (left). Time evolution of spot multiplication. This figure was produced in a 256 by 256 simulation with physical dimensions of 0.5 by 0.5 and a time step of 0.01. The times t at which the figures were taken are as follows: (**A**) $t = 0$; (**B**) $t = 350$; (**C**) $t = 510$; and (**D**) $t = 650$.
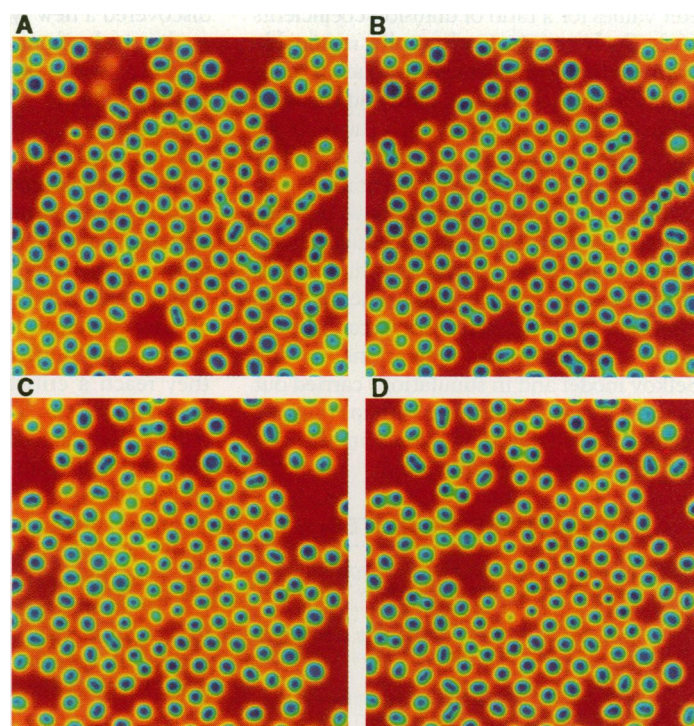

Fig. 5 (right). Time evolution of pattern ε. The images are 250 time units apart. In the corners (which map to the same point in physical space), one can see a yellow region in (**A**) to (**C**). It has decayed to red in (**D**). In (A) and (B), the center of the left border has a red region that is nearly filled in (D).

formation cannot occur in systems in which all diffusion coefficients are equal. [For a comprehensive discussion of these issues, see Pearson and co-workers (10, 11); for a discussion of Turing instabilities in the model at hand, see Vastano et al. (12).] The only Turing patterns that can occur bifurcate off the nontrivial steady uniform state (the blue state). Most of the patterns discussed in this report occur for parameter values such that the nontrivial steady state does not exist. With the ratio of diffusion coefficients used here, Turing patterns occur only in a narrow parameter region in the vicinity of $F = k = 0.0625$, where the line of saddle-node bifurcations coalesces with the line of Hopf bifurcations. In the vicinity of this point, the branch of small-amplitude Turing patterns is unstable (12).

With equal diffusion coefficients, no patterns formed in which small asymmetries in the initial conditions were amplified by the dynamics. This observation can probably be understood in terms of the following fact: Nonlinear plane waves in two dimensions cannot be destabilized by diffusion in the case that all diffusion coefficients are equal (13). During the initial stages of the evolution, the corners of the square perturbation are rounded off. The perturbation then evolves as a radial wave, either inward or outward depending on the parameter values. Such a wave cannot undergo spontaneous symmetry breaking unless the diffusion coefficients are unequal. However, I found symmetry breaking over a wide range of parameter values for a ratio of diffusion coefficients of 2. Such a ratio is physically reasonable even for small molecules in aqueous solution. Given this diffusion ratio and the wide range of parameters over which the replicating spot patterns exist, it is likely that they will soon be observed experimentally.

Recently Hasslacher et al. have demonstrated the plausibility of subcellular chemical patterns through lattice-gas simulations of the Selkov model (14). The patterns discussed in the present article can also be found in lattice-gas simulations of the Selkov model and in simulations carried out in three space dimensions. Perhaps they are related to dynamical processes in the cell such as centrosome replication.

REFERENCES AND NOTES

1. G. Nicolis and I. Prigogine, *Self-Organization in Non-Equilibrium Systems* (Wiley, New York, 1977).
2. E. E. Selkov, *Eur. J. Biochem.* **4**, 79 (1968).
3. P. Gray and S. K. Scott, *Chem. Eng. Sci.* **38**, 29 (1983); *ibid.* **39**, 1087 (1984); *J. Phys. Chem.* **89**, 22 (1985).
4. J. A. Vastano, J. E. Pearson, W. Horsthemke, H. L. Swinney, *Phys. Lett. A* **124**, 6 (1987). *ibid.*, p. 7; *ibid.*, p. 320.
5. K. J. Lee, W. D. McCormick, Q. Ouyang, H. L. Swinney, *Science* **261**, 192 (1993).
6. P. Hohenberg and M. Cross, *Rev. Mod. Phys.* **65**, 3 (1993).
7. J. Guckenheimer and P. Holmes, *Nonlinear Oscillations, Dynamical Systems, and Bifurcations of Vector Fields* (Springer-Verlag, Berlin, 1983), chap. 3.
8. Y. Kuramoto, *Chemical Oscillations, Waves, and Turbulence* (Springer-Verlag, Berlin, 1984).
9. A. Kawczynski, W. Comstock, R. Field, *Physica D* **54**, 220 (1992); A. Hagberg and E. Meron, University of Arizona preprint.
10. J. E. Pearson and W. Horsthemke, *J. Chem. Phys.* **90**, 1588 (1989).
11. J. E. Pearson and W. J. Bruno, *Chaos* **2**, 4 (1992); *ibid.*, p. 513.
12. J. A. Vastano, J. E. Pearson, W. Horsthemke, H. L. Swinney, *J. Chem. Phys.* **88**, 6175 (1988).
13. J. E. Pearson, *Los Alamos Publ. LAUR 93-1758* (Los Alamos National Laboratory, Los Alamos, NM, 1993).
14. B. Hasslacher, R. Kapral, A. Lawniczak, *Chaos* **3**, 1 (1993).
15. I am happy to acknowledge useful conversations with S. Ponce-Dawson, W. Horsthemke, K. Lee, L. Segel, H. Swinney, B. Reynolds, and J. Theiler. I also thank the Los Alamos Advanced Computing Laboratory for the use of the Connection Machine and A. Chapman, C. Hansen, and P. Hinker for their ever-cheerful assistance with the figures.

Pattern Formation by Interacting Chemical Fronts

Kyoung J. Lee, W. D. McCormick, Qi Ouyang, Harry L. Swinney*

Experiments on a bistable chemical reaction in a continuously fed thin gel layer reveal a new type of spatiotemporal pattern, one in which fronts propagate at a constant speed until they reach a critical separation (typically 0.4 millimeter) and stop. The resulting asymptotic state is a highly irregular stationary pattern that contrasts with the regular patterns such as hexagons, squares, and stripes that have been observed in many nonequilibrium systems. The observed patterns are initiated by a finite amplitude perturbation rather than through spontaneous symmetry breaking.

In recent years, pattern formation has become a very active area of research, motivated in part by the realization that there are many common aspects of patterns formed by diverse physical, chemical, and biological systems and by cellular automata and differential equation models. In experiments on a chemical system, we have discovered a new type of pattern that differs qualitatively from the previously studied chemical waves [rotating spirals (1)], stationary "Turing" patterns (2–4), and chaotic patterns (5). These new patterns form only in response to large-amplitude perturbations—small-amplitude perturbations decay. A large perturbation evolves into an irregular pattern that is stationary (time-independent) (Fig. 1). The patterns have a length scale determined by the interaction of the chemical fronts, which propagate toward one another at constant speed until they reach a critical distance and stop, as Fig. 2 illustrates. The growth of these front patterns is markedly different from Turing patterns: The front patterns develop locally and spread to fill space, as in crystal growth, whereas Turing patterns emerge spontaneously everywhere when the critical value of a control parameter is exceeded.

The front patterns are highly irregular, in contrast with Turing patterns, which emerge as a regular array of stripes or hexagons (in two-dimensional systems) at the

transition from a uniform state (4). The interaction of fronts illustrated in Fig. 2 also contrasts with the behavior in excitable chemical media, where colliding fronts annihilate one another (1), and with solitons, where nonlinear waves pass through one another (6).

Our experiments have been conducted using an iodate-ferrocyanide-sulfite reaction, which is known to exhibit bistability and large oscillations in pH in stirred flow reactors (7). The other reactions that yield stationary chemical patterns are the well-studied chlorite-iodide-malonic acid reaction (3–5) and a variant reaction (8) that uses chlorine dioxide instead of chlorite. We chose the iodate-ferrocyanide-sulfite reaction as a new candidate for studies of pattern formation because a pH indicator could be used to visualize patterns that might form.

The following experiments illustrate the differences between our patterns and those previously observed in reaction-diffusion systems. A diagram of the gel disc reactor is shown in Fig. 3. Gel-filled reactors were developed several years ago (9) to study reaction-diffusion systems maintained in well-defined states far from equilibrium. These reactors are now widely used for studying sustained patterns that arise solely from the interplay of diffusion and chemical kinetics—the gel prevents convective motion. A thin polyacrylamide gel layer (0.2 mm thick, 22 mm in diameter) is fed diffusively by a continuously refreshed reservoir of chemicals (10). There are two thin membranes between the polyacrylam-

Center for Nonlinear Dynamics and the Department of Physics, University of Texas at Austin, Austin, TX 78712.

*To whom correspondence should be addressed.